

## Grain growth kinetic in $x\text{TiO}_2$ –6 wt.% $\text{Bi}_2\text{O}_3$ –(94 – $x$ ) ZnO ( $x=0, 2, 4$ ) ceramic system

Senol Yilmaz · Ediz Ercenk · H. Ozkan Toplan ·  
Volkan Gunay

Received: 31 October 2005 / Accepted: 15 June 2006 / Published online: 23 February 2007  
© Springer Science+Business Media, LLC 2007

**Abstract** The grain growth kinetics in the 0, 2 and 4 wt.%  $\text{TiO}_2$  added ZnO–6 wt.%  $\text{Bi}_2\text{O}_3$  system was studied using the simplified phenomenological grain growth kinetics equation  $G^n = k \cdot t \cdot \exp(-Q/R \cdot T)$  together with the physical properties of the sintered samples. The grain growth exponent value ( $n$ ) and the apparent activation energy for the ZnO–6 wt.%  $\text{Bi}_2\text{O}_3$  system was 5 and 218 kJ/ mol, respectively. The addition of the  $\text{TiO}_2$  to the ZnO–6 wt.%  $\text{Bi}_2\text{O}_3$  system inhibited the ZnO grain growth. At 2 and 4 wt.%  $\text{TiO}_2$  additions, the apparent activation energies were calculated as 467 and 346 kJ/ mol, respectively. The addition of  $\text{TiO}_2$  to the system inhibited the grain growth of ZnO ceramics.

### Introduction

ZnO based varistor ceramics have technological importance because of their highly non-linear current–voltage characteristics enabling them to be used as reversible, solid state switches with large energy-handling capabilities [1].

Commercial ZnO ceramics varistors are compositionally designed to contain several metal oxides,

which modify the sintering and electrical properties of these unique electrical ceramics. Additives may include  $\text{Bi}_2\text{O}_3$ ,  $\text{Pr}_6\text{O}_{11}$ ,  $\text{Sb}_2\text{O}_3$ ,  $\text{Cr}_2\text{O}_3$ ,  $\text{SiO}_2$ ,  $\text{CoO}/\text{Co}_3\text{O}_4$ ,  $\text{MnO}/\text{MnO}_2$  and other oxides, each of which makes specific contributions to the microstructural evolution of the ZnO during sintering as well as to the electrical characteristics of the sintered ZnO ceramic varistor. Since the electrical properties of these polycrystalline ceramics are directly depend on the microstructure as the grain size effect the varistor voltage per unit thickness. Other properties of polycrystalline ceramics also depend on microstructure, so that it is important in a general sense to fundamentally understand to microstructural development of ZnO ceramics. Therefore, it is important to study in a systematic way the effect of these additives to the microstructural development and to the grain growth kinetics of the materials [2].

$\text{Bi}_2\text{O}_3$  carries a special importance since it enhances the grain growth and effects the stability of the non-linear current–voltage characteristics of the material. Among the numerous work published on the subject, Senda and Bradt [3], presented the most detailed study covering the grain growth kinetics in ZnO ceramics containing up to 4 wt.%  $\text{Bi}_2\text{O}_3$ . In their work, Senda and Bradt [3] used simplified grain growth kinetics equation

$$G^n = k \cdot t \cdot \exp(-Q/R \cdot T), \quad (1)$$

where  $G$  is the average grain size at time  $t$ ,  $n$  is the kinetic grain growth exponent value,  $K$  is a constant,  $Q$  is the apparent activation energy,  $R$  is the gas constant and  $T$  is the absolute temperature. Using this equation, Senda and Bradt have calculated the grain growth

S. Yilmaz (✉) · E. Ercenk · H. O. Toplan  
Engineering Faculty, Sakarya University, Esentepe,  
Sakarya, Turkey  
e-mail: symaz@sakarya.edu.tr

V. Gunay  
Materials Institute, TUBITAK-MRC, P. O. Box 21,  
41470 Gebze, Turkey

exponent value ( $n$ ) as three apparent activation energy ( $Q$ ) as  $224 \pm 16$  kJ/mol in the sintering of the pure ZnO system. However, Dey and Bradt [4] found that the rate of grain growth of ZnO was affected by the increased amounts of  $\text{Bi}_2\text{O}_3$  addition (from 3 to 12 wt.%) and the apparent activation energy for the grain growth of system was raised from 160 to 270 kJ/mol, respectively. They attributed this to the change of the grain growth mechanism from the phase-boundary reaction in the liquid phase process for low  $\text{Bi}_2\text{O}_3$  contents ( $\leq 5$ –6 wt.%) to that of ion diffusion controlled mechanism in a liquid phase.

ZnO–6 wt.%  $\text{Bi}_2\text{O}_3$  system was chosen on the base composition by our group to study the effects of various oxide additives on the grain growth kinetics. The additions of MnO [5] and CoO [2] to the ZnO–6 wt.%  $\text{Bi}_2\text{O}_3$  system were studied and already published and this present work is the continuation of the previous works in the grain growth kinetics of the ZnO varistors. The aim of the present work is to study the grain growth kinetics of ZnO containing 6 wt.%  $\text{Bi}_2\text{O}_3$  which was found to be critical level in the change of the grain growth kinetics. A further aim of the work is also to study the effect of  $\text{TiO}_2$  additions as a third component to the microstructure and to the sintering behaviour of the system.

## Experimental procedure

High purity ZnO (99.7%, Metal Bilesikleri A.S., Gebze, Turkey),  $\text{Bi}_2\text{O}_3$  and  $\text{TiO}_2$  powders from Merck (pure grade) were used in preparation of three basic compositions; ZnO–6 wt.%  $\text{Bi}_2\text{O}_3$  and those containing 2 and 4 wt.%  $\text{TiO}_2$ . ZnO powders revealed a needle like fine crystal ca.  $0.5 \mu\text{m}$  width and ca.  $0.5$ – $2 \mu\text{m}$  length. The calculated amounts of oxides for the indicated compositions were ball milled in ashless rubber lined ceramics jars for 6 h using zirconia balls and distilled water as the milling media. The mixture were dried to ca. 10–15% moisture level and then granulated. Samples of 10 mm diameter and ca. 8 mm thick were prepared by semi-dry pressing of the granules of  $-150 \mu\text{m}$  to  $+75 \mu\text{m}$  in size at a pressure of 100 MPa. The specimens were sintered at 1,000, 1,100, 1,200 and 1,300 °C for 1, 3, 5 and 10 h using a heating rate of 5 °C/min. and were naturally cooled in a PID controlled furnace.

The bulk densities of the samples were calculated from their weights and dimensions. Characterizations of the phases in the sintered specimens were carried out by X-ray diffraction using  $\text{CuK}_\alpha$  radiation. For the microstructural observations both scanning electron

microscopy (SEM) of the fracture surfaces and optical microscopy of polished and etched (in a 50% hydrochloric acid–distilled water solution) surfaces were used. Grain size measurements were carried out on the micrographs of the etched samples using the following equation

$$G = 1.56 \cdot \bar{L}, \quad (2)$$

where  $G$  is the average grain size,  $\bar{L}$  is the average grain boundary intercept length of four random lines on two different micrographs of each sample [6].

## Results and discussion

### Physical properties of the sintered samples

Pellets sintered at different temperatures were examined by X-ray diffraction. Presence of  $\text{Bi}_4\text{Ti}_3\text{O}_{12}$  (ASTM No: 12-213) and ZnO (ASTM No: 5-0664) phases has been detected in samples fired at 1,000 °C, but  $\text{Bi}_4\text{Ti}_3\text{O}_{12}$  disappears after firing at 1,100 °C and is accompanied by formation of  $\text{Zn}_2\text{TiO}_4$  spinel. Therefore, ZnO,  $\beta$ - $\text{Bi}_2\text{O}_3$  and  $\text{Zn}_2\text{TiO}_4$  (ASTM card No: 5-0664, 27-50 and 18-1487, respectively) are present in the samples fired at 1,100 °C and over. These results are consistent with those of Suzuki and Bradt [7]. Sun and Kim [8] and Toplan and Karakas [9] have also reported that during the beginning of the liquid phase sintering process in the ZnO– $\text{Bi}_2\text{O}_3$ – $\text{TiO}_2$  system, the  $\text{TiO}_2$  rapidly dissolves in the  $\text{Bi}_2\text{O}_3$ -rich liquid and reacts to form  $\text{Bi}_4\text{Ti}_3\text{O}_{12}$  according to

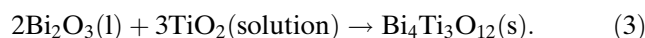
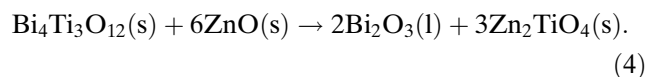


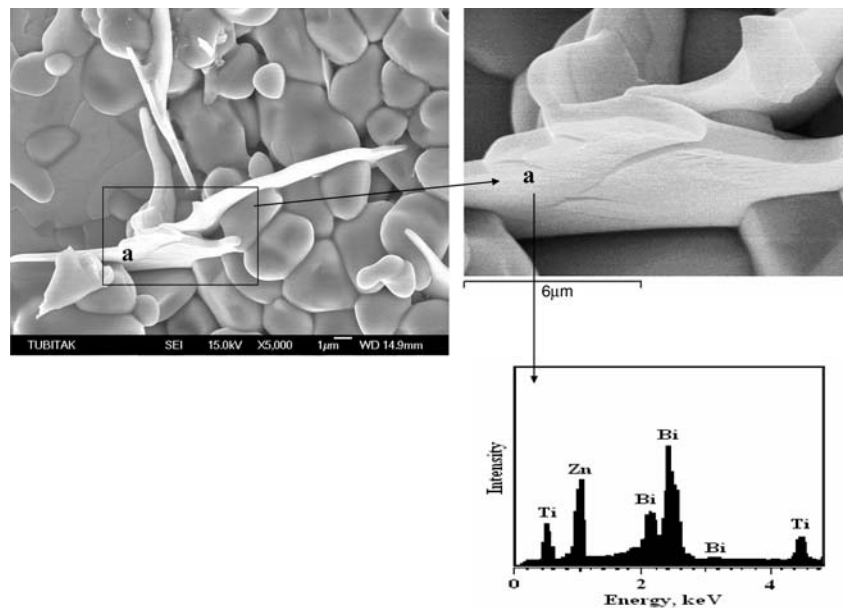
Figure 1 is a higher magnification scanning electron microscope (SEM) image of a sample sintered for 1 h at 1,000 °C revealing white  $\text{Bi}_4\text{Ti}_3\text{O}_{12}$  phase located on the dark grey ZnO grains as confirmed by energy dispersive spectroscopy (EDS). The solid  $\text{Bi}_4\text{Ti}_3\text{O}_{12}$  is than reported to decompose and react with the solid ZnO grains at 1,050 °C, according to the reaction [8, 9]



This latter reaction yields the  $\text{Zn}_2\text{TiO}_4$  spinel phase. The reactivity of the  $\text{Bi}_2\text{O}_3$ -rich liquid towards the solid ZnO grains may be enhanced by formation of the  $\text{Bi}_4\text{Ti}_3\text{O}_{12}$  [7].

The presence of  $\text{Bi}_2\text{O}_3$  in  $\beta$ -form is in agreement with the result of Cerva and Russwurm [10], Ozkan

**Fig. 1** SEM image and EDS analyses of ZnO–6 wt.% Bi<sub>2</sub>O<sub>3</sub>–2 wt.% TiO<sub>2</sub> system sintered 1 h at 1,000 °C (a is liquid phase containing Zn, Ti, Bi)



et al. [5] and Gunay et al. [2]. At 1,300 °C there was no peaks indicating of  $\beta$ -Bi<sub>2</sub>O<sub>3</sub> due to volatilization of some this phase.

The weight loss data was determined by weighing the green-pressed pellets before and after heating to the indicated temperatures by employing the same heating rate used in sintering and 1 h soaking time. It was observed that all samples showed the decrease in weight with increasing sintering temperatures and also

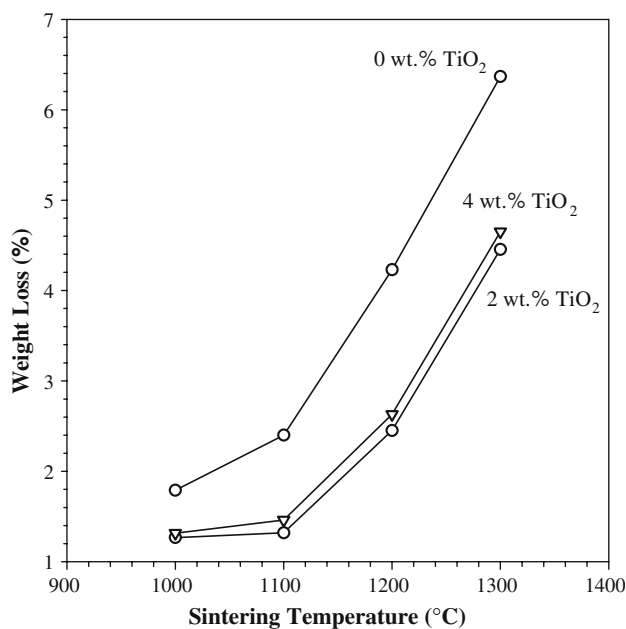


**Fig. 2** Weight losses of the samples with increasing sintering temperatures for 1 h

with increasing sintering time. Weight losses of samples with different TiO<sub>2</sub> contents against sintering temperatures are shown in Fig. 2.

There was a sharp increase in weight losses of undoped TiO<sub>2</sub> above 1,100 °C and this was attributed to the change of volatilization behaviour of Bi<sub>2</sub>O<sub>3</sub> at high temperature as reported by Wong [11]. In Fig. 2, the total weight loss of TiO<sub>2</sub> free sample sintered at 1,300 °C is about 6.3%. This was not only from the loss of Bi<sub>2</sub>O<sub>3</sub>, but also these should be some losses from volatilization of ZnO over 1,300 °C as reported in the literature by Wong [11]. The addition TiO<sub>2</sub> to the system decreases the weight loss, this could be attributed the formation of Bi<sub>4</sub>Ti<sub>3</sub>O<sub>12</sub> phase.

The bulk density data given in Fig. 3 shows the effect of sintering temperatures (1,000 and 1,300 °C), sintering times (1, 3, 5 and 10 h) and the TiO<sub>2</sub> content on the densification of the ZnO–6 wt.% Bi<sub>2</sub>O<sub>3</sub> system. However, the SEM micrographs of the fracture of samples with 0, 2 and 4 wt.% TiO<sub>2</sub> content sintered at 1,100 °C for 1 h were compared in Fig. 4a–c. Higher sintering temperatures and longer sintering times gave rise to a reduction in bulk density due to increased amount of porosity between and within the large grains of ZnO resulting from the rapid grain growth induced by the liquid phase sintering and also by the losses Bi<sub>2</sub>O<sub>3</sub> especially at sintering over 1,100 °C. The porous microstructure can be seen from the micrographs given in Fig. 4a, for the ZnO–6 wt.% Bi<sub>2</sub>O<sub>3</sub> system. The highest densification is obtained at low sintering temperature due to the liquid phase sintering; in this case 1,000 °C for the samples with 2 wt.% TiO<sub>2</sub> addition

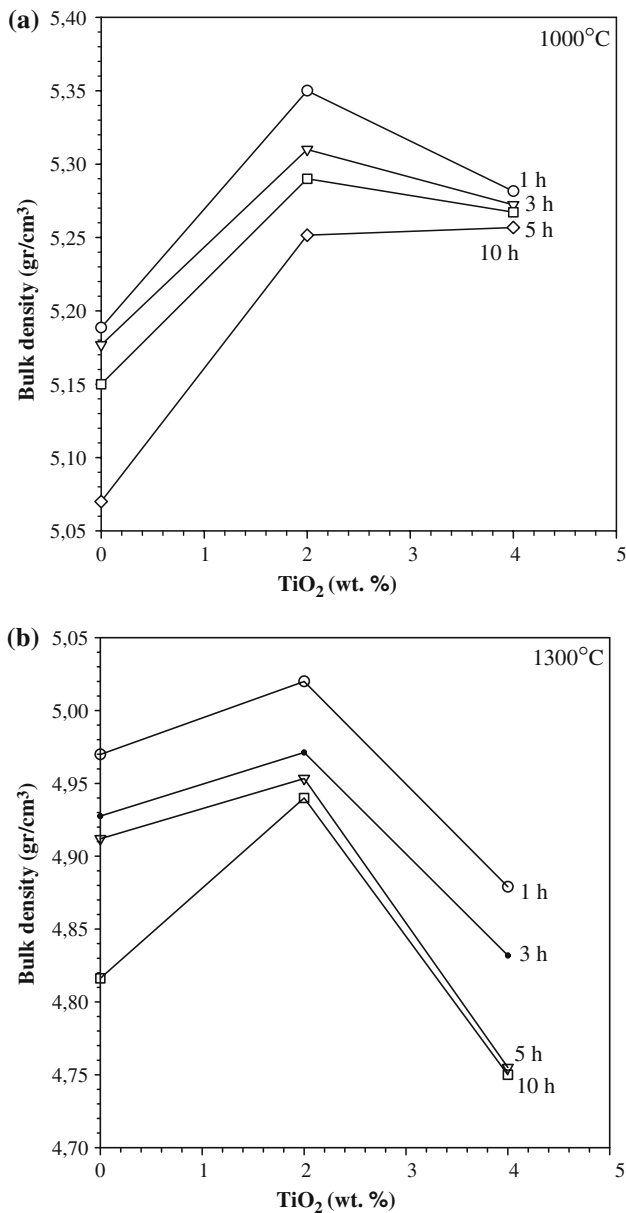


**Fig. 3** The effects of TiO<sub>2</sub> content and sintering times on bulk densities of samples sintered at (a) 1,000 °C and (b) 1,300 °C

(Fig. 4b). As shown in Fig. 2, Bi<sub>2</sub>O<sub>3</sub> losses are lowest at this composition because of dissolving TiO<sub>2</sub> in the Bi<sub>2</sub>O<sub>3</sub> and formation Bi<sub>4</sub>Ti<sub>3</sub>O<sub>12</sub> phases at this temperature. The addition of 4 wt.% TiO<sub>2</sub> also results in a reduction in the bulk densities of the samples sintered at 1,000 and 1,300 °C. Since, this reduction mainly arises from the differences in the densities of ZnO (5.68 g/cm<sup>3</sup>) and that of TiO<sub>2</sub> (Rutile, 4.27 g/cm<sup>3</sup>). However, in sintering at 1,300 °C the optimum densification is attained in 2 wt.% TiO<sub>2</sub>-added samples, mainly due to the reduction of intergranular porosity (Fig. 4c).

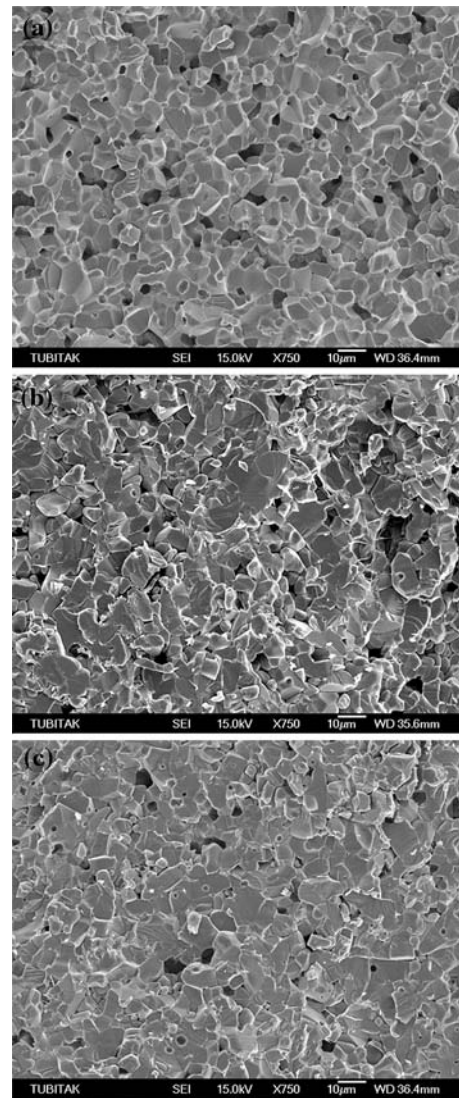


**Fig. 4** The SEM micrographs of the fracture of samples with (a) 0 wt.%, (b) 2 wt.% and (c) 4 wt.%TiO<sub>2</sub> content sintered at 1,100 °C for 1 h

### Grain growth kinetics

The optical micrographs (Fig. 5a–f) were taken from the polished and etched surfaces of the samples which were sintered for 3 h at 1,100 and 1,300 °C. Grain sizes are given in Table 1. Grain size and grain growth kinetics were obtained from Fig. 5a–f. The possible reason of the smaller grain sizes after sintering at 1,300 °C for 3 h could be that the inhibiting role of the ZnTiO<sub>4</sub> spinel phase as seen in Fig. 5f. Also, there are spinel grains together with ZnO grains and the overall grain size were measured as 28.18, 35.88 and 21.06 µm, respectively, for 0, 2 and 4 wt.% TiO<sub>2</sub> content sintered at 1,300 °C for 3 h. This behaviour was observed at all the sintering times and temperatures. As a result, the

**Fig. 5** Optical photographs polished and etched surfaces of ZnO–6 wt.% Bi<sub>2</sub>O<sub>3</sub> (a) 0 wt.%, (b) 2 wt.% and (c) 4 wt.% TiO<sub>2</sub> at 1,100 °C–3 h, (d) 0 wt.%, (e) 2 wt.% and (f) 4 wt.% TiO<sub>2</sub> at 1,300 °C–3 h

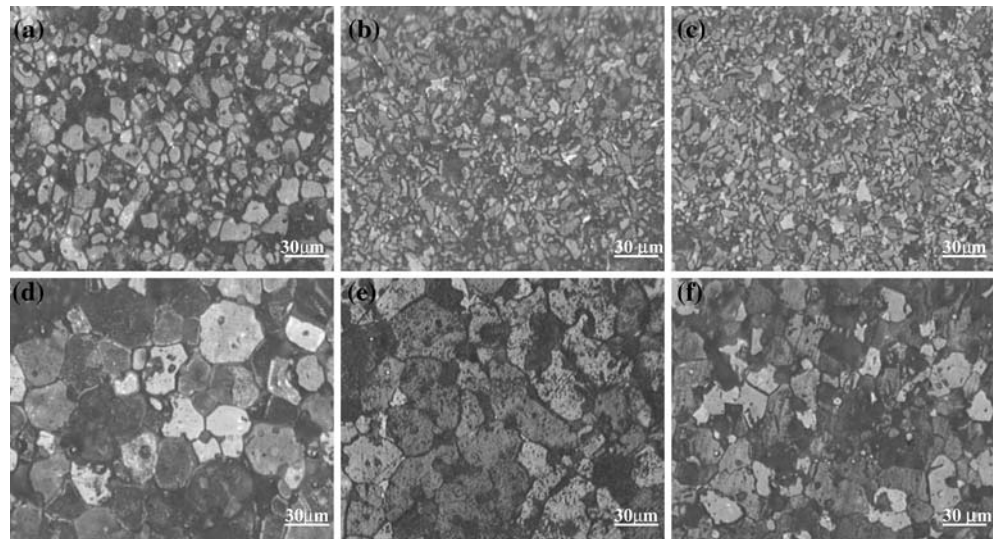


**Table 1** Grain sizes of the sintered samples

Sin. Tem. → Sin. Time ↓	Grain size (μm)								
	1,100 °C ZnO–6 wt.% Bi <sub>2</sub> O <sub>3</sub> –0 wt.% TiO <sub>2</sub>	1,200 °C ZnO–6 wt.% Bi <sub>2</sub> O <sub>3</sub> –2 wt.% TiO <sub>2</sub>	1,300 °C ZnO–6 wt.% Bi <sub>2</sub> O <sub>3</sub> –4 wt.% TiO <sub>2</sub>	1,100 °C ZnO–6 wt.% Bi <sub>2</sub> O <sub>3</sub> –2 wt.% TiO <sub>2</sub>	1,200 °C ZnO–6 wt.% Bi <sub>2</sub> O <sub>3</sub> –4 wt.% TiO <sub>2</sub>	1,300 °C ZnO–6 wt.% Bi <sub>2</sub> O <sub>3</sub> –4 wt.% TiO <sub>2</sub>	1,100 °C ZnO–6 wt.% Bi <sub>2</sub> O <sub>3</sub> –4 wt.% TiO <sub>2</sub>	1,200 °C ZnO–6 wt.% Bi <sub>2</sub> O <sub>3</sub> –4 wt.% TiO <sub>2</sub>	1,300 °C ZnO–6 wt.% Bi <sub>2</sub> O <sub>3</sub> –4 wt.% TiO <sub>2</sub>
1	14.03	15.84	21.36	13.25	14.81	31.97	13.25	15.91	23.39
3	17.15	21.83	28.18	14.04	20.28	35.88	14.04	17.31	21.06
5	17.15	21.83	31.62	15.59	21.06	38.06	15.91	18.71	31.98
10	23.39	25.73	35.88	19.49	24.95	42.12	18.71	21.84	31.98

inhibiting role of the spinel phase is one of the reasons, and also the sizes of spinel phases which were also measured especially at higher temperature, such as 1,300 °C with high TiO<sub>2</sub> content. As seen in Fig. 6, ceramic system sintered at 1,300 °C for 3 h with 2 wt.% TiO<sub>2</sub> addition. There are too many spinel phases (ZnTiO<sub>4</sub>) in between ZnO grains. These phases

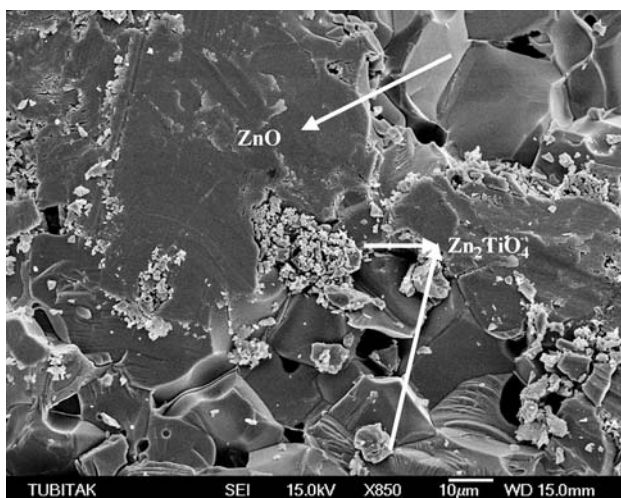


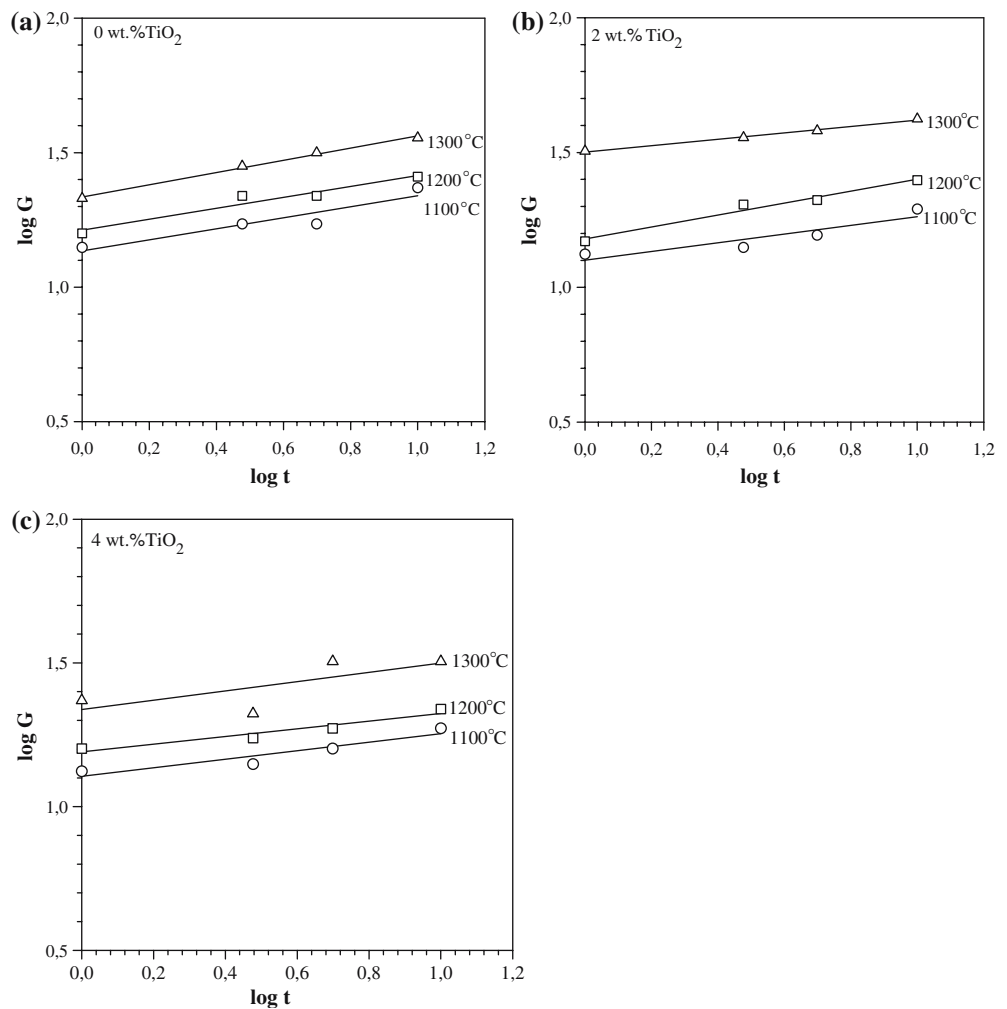
**Fig. 6** SEM micrograph of the fracture surface of the sample with 2 wt.% TiO<sub>2</sub> sintered at 1,300 °C for 3 h

are not clearly visible in optical micrographs, but during the grain size counting these spinel phases counted as grains together with ZnO grains. As seen in Fig. 6, spinel phases are very small compared to ZnO grains. Spinel phases increased with increasing TiO<sub>2</sub> content and also with increasing sintering time and temperatures. As shown in the microstructure (Fig. 5a–f) that the addition of TiO<sub>2</sub> to ZnO–6 wt.% Bi<sub>2</sub>O<sub>3</sub> system decrease the grains size. The grain growth kinetics can be determined using the simplified phenomenological kinetics (Eq. 1). The grain growth exponent value ( $n$ ) in the equation can be found at isothermal conditions where the kinetic equation is expressed in the form of

$$n \log G = \log t + [\log K_0 - 0.434 \cdot (Q/R \cdot T)]. \quad (5)$$

The  $n$  value can be calculated from the slope of the log (grain size) vs. log (time) line plot which is equal to  $(1/n)$ . Such plots were made for isothermal conditions employed at the sintering temperatures and the ( $n$ ) values were calculated from the slopes of the plots constructed by the linear regression method. Figure 7a–c depicts the log  $G$  vs. log  $t$  plots for different TiO<sub>2</sub> contents at the different sintering temperatures. Calculated ( $n$ ) values are listed in Table 2.

**Fig. 7** Isothermal grain growth of ZnO–6 wt.% Bi<sub>2</sub>O<sub>3</sub> ceramics containing (a) 0 wt.% TiO<sub>2</sub>, (b) 2 wt.% TiO<sub>2</sub> and (c) 4 wt.% TiO<sub>2</sub> at different sintering temperatures



The average grain growth exponent value of 5, determined for ZnO–6 wt.% Bi<sub>2</sub>O<sub>3</sub> system is the same to the values obtained by Gunay et al [2], Senda and Bradt [3] and Dey and Bradt [4]. The addition of 2 and 4 wt.% TiO<sub>2</sub> gave the values “*n*” 6 and 7, respectively.

When Eq. 1 is expressed in the form

$$\log(G^n/t) = \log K_0 - (0.434 \cdot Q/R) \cdot (1/T) \tag{6}$$

the apparent activation energy (*Q*) for the grain growth process can be calculated from the gradient of the Arrhenius plot of log (*G<sup>n</sup>/t*) vs. (1/*T*). Such plot were constructed for the system studied are shown in Fig. 8a–c and the calculated apparent activation energies along with the logarithm of the pre-exponential constant *K*<sub>0</sub> are also listed in Table 2.

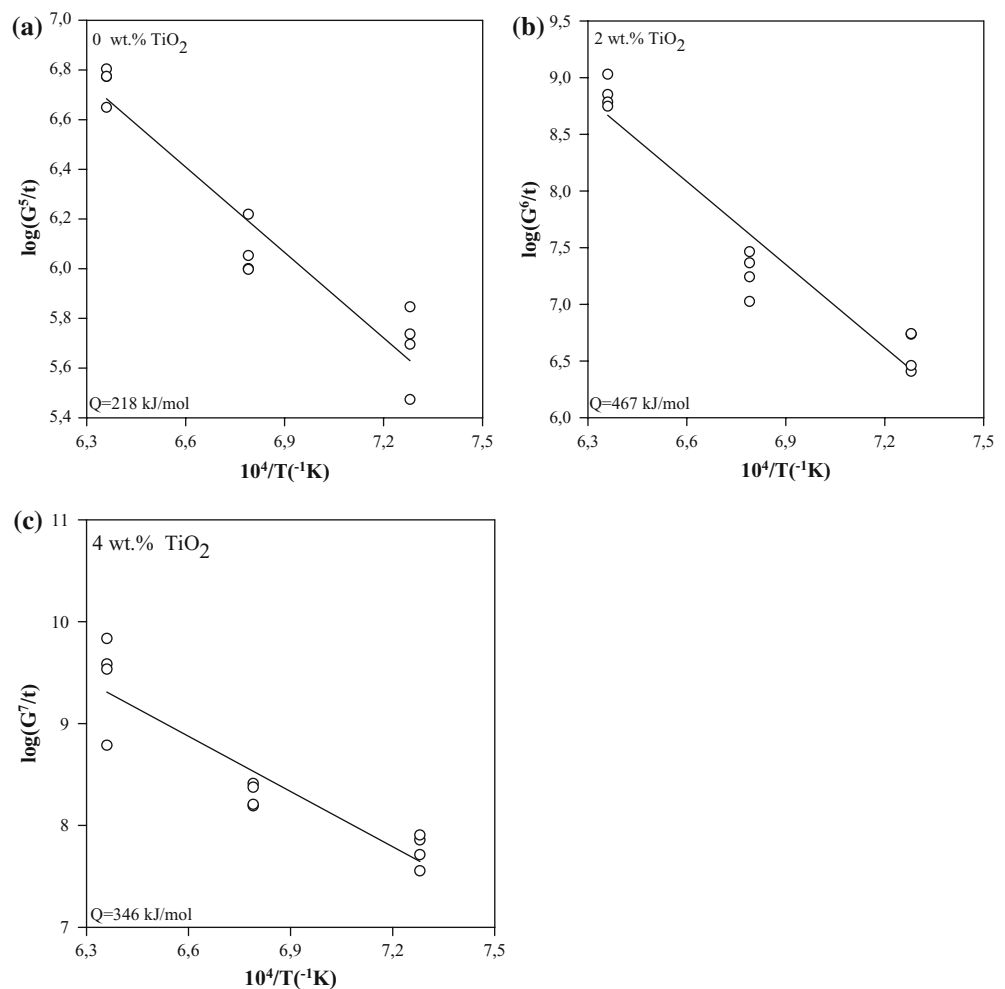
The numerous studies on the grain growth kinetics of ZnO have revealed that the rate-controlling mechanism is the solid-state diffusion of Zn<sup>2+</sup> cations. The apparent activation energy for this process is about 225 kJ/mol, whereas, the studies on the ZnO–Bi<sub>2</sub>O<sub>3</sub>

system showed that the grain growth of ZnO proceeds in liquid phase of Bi<sub>2</sub>O<sub>3</sub> by mechanism of solution–precipitation at phase boundaries [3, 4, 11]. Among these studies, the notable work of Senda and Bradt [2] showed that low level of Bi<sub>2</sub>O<sub>3</sub> addition (~0.5 wt.%) to ZnO reduced the apparent activation energy to 150 kJ/mol and further additions up to 4 wt.% did not have a pronounced affect on the apparent activation energy. However, in latter work by Dey and Bradt [4] showed the addition of Bi<sub>2</sub>O<sub>3</sub> beyond this level increased the apparent activation energy gradually and 274 kJ/mol was found for the 12 wt.% Bi<sub>2</sub>O<sub>3</sub> addition. They also

**Table 2** Calculated grain growth exponent (*n*), apparent activation energy (*Q*) and pre-exponential constant (*K*<sub>0</sub>) values

TiO <sub>2</sub> (wt.%)	<i>n</i> Values used in Arrhenius plots	Log <i>K</i> <sub>0</sub>	<i>Q</i> (kJ/ mol)
0	5	13.97	218
2	~6	24.19	467
4	~7	20.80	346

**Fig. 8** Arrhenius plots for the grain growth of ZnO–6 wt.% Bi<sub>2</sub>O<sub>3</sub> system with (a) 0 wt.% TiO<sub>2</sub>, (b) 2 wt.% TiO<sub>2</sub> and (c) 4 wt.% TiO<sub>2</sub> additions



showed that this increase in the activation energy was due to change of grain growth mechanism from the phase-boundary reaction in a liquid-phase sintering to that of a ion diffusion mechanism in a thicker layer of liquid phase. They also proposed that this change became effective for the additions of ca. 5–6 wt.% Bi<sub>2</sub>O<sub>3</sub>.

In this study the apparent activation energy of the ZnO–6 wt.% Bi<sub>2</sub>O<sub>3</sub> system was calculated as 218 kJ/mol. This value agrees with the value of 232 kJ/mol quoted for same composition by Day and Bradt [4] and 200 kJ/mol quoted by Ozkan et al. [5] and by Gunay et al. [2].

The apparent activation energy of the ZnO–6 wt.% Bi<sub>2</sub>O<sub>3</sub> ceramic system with the addition of 2 and 4 wt.% TiO<sub>2</sub>, were calculated as 467 and 346 kJ/mol, respectively. The effects of TiO<sub>2</sub> additions (above 1 wt.%) on ZnO grain growth during liquid-phase sintering are distinctly same with those of the other two spinel-forming additives, Sb<sub>2</sub>O<sub>3</sub> [12] and Al<sub>2</sub>O<sub>3</sub> [13]. With increasing Sb<sub>2</sub>O<sub>3</sub> and Al<sub>2</sub>O<sub>3</sub>

levels, which cause increasing Zn<sub>7</sub>Sb<sub>2</sub>O<sub>12</sub> and ZnAl<sub>2</sub>O<sub>4</sub> spinel formation, the ZnO grain size continually decreases. Result of the present study showed that the addition of 2 wt.% TiO<sub>2</sub> (or above) inhibited the ZnO grain growth by formation of Zn<sub>2</sub>TiO<sub>4</sub> spinel phase. This result is in agreement with the literature [14, 15].

As explained in the grain size measurement, the formation of spinel phases and their contribution influence the main grain size measurements. The apparent activation energy of the ZnO–6 wt.% Bi<sub>2</sub>O<sub>3</sub> ceramic system with the addition of 4 wt.% TiO<sub>2</sub> was calculated lower than with the addition of 2 wt.% TiO<sub>2</sub>. The reason for this was the overall size of 4 wt.% TiO<sub>2</sub> system.

## Conclusions

The effect of TiO<sub>2</sub> additions of 0–4 wt.% to the sintering behaviour and to the grain growth mechanism

of the ZnO–6 wt.% Bi<sub>2</sub>O<sub>3</sub> system was studied. The highest densification was found at 1,000 °C with 2 wt.% TiO<sub>2</sub> addition. At higher sintering temperatures and longer sintering times, the bulk densities were decreased mainly due to volatilization of Bi<sub>2</sub>O<sub>3</sub>. The grain growth exponent value of 5 and the apparent activation energy of 218 kJ/mol found for the system with no addition of TiO<sub>2</sub>, showed good correlation with the published data for the grain growth mechanism of the diffusion-controlled process in liquid phase sintering. The addition TiO<sub>2</sub> to the system raised the grain growth exponent value to 6 and 7. The apparent activation energies with the addition of 2 and 4 wt.% TiO<sub>2</sub> were calculated as 467 and 346 kJ/mol, respectively. It could be concluded that Zn<sub>2</sub>TiO<sub>4</sub> spinel phase reduced the ZnO grain boundary mobility by a particle drag mechanism. This resulted with inhibiting the grain growth of ZnO.

## References

1. Toplan HO, Erkalfa H, Ozkan OT (2003) *Cer Silikat* 47(3):116
2. Gunay V, Gelecek-Sulan O, Ozkan OT (2004) *Cer Int* 30:105
3. Senda T, Bradt RC (1990) *J Am Cer Soc* 73(1):106
4. Dey D, Bradt RC (1992) *J Am Cer Soc* 75(9):2529
5. Ozkan OT, Avcı M, Oktay E, Erkalfa H (1988) *Cer Int* 24:151
6. *Metals handbooks*, vol. 8, 8th edn., Newby JR (Coordinator), Davis JR (Senior Technical Editor), Am. Soc. for Metals, PA, USA (1973)
7. Suzuki H, Bradt RC (1995) *J Am Cer Soc* 78(5):1354
8. Sun GY, Kim CH (1988) *Adv Cer Mat* 3(6):604
9. Toplan HO, Karakas Y (2002) *Cer Int* 28:911
10. Cerva H, Russwurm W (1988) *J Am Cer Soc* 71(7):522
11. Wong J (1989) *J Appl Phys* 51(8):1541
12. Chen Y-C, Shen C-Y, Chen H-Z, Wey Y-F, Wu L (1991) *Jap J Appl Phys* 30(1):84
13. Nunes SI, Bradt RC (1995) *J Am Cer Soc* 78(9):2469
14. Tronjtel M, Kolar D, Karasevec V, Yan MF, Heuer AH (eds) (1990) *Adv. in Cer.*, vol. 7. Am. Cer. Soc
15. Peygney A, Andryanjatovo H, Legros R, Rousset A (1992) *J Mater Sci* 27:2397